Reflectivity of the quantum grating and the grating polariton

F. Tassone
Institut de Physique Théorique, Ecole Polytechnique Fédérale de Lausanne PHB Ecublens, CH-1015 Lausanne, Switzerland

F. Bassani
Scuola Normale Superiore, piazza dei Cavalieri 7, I-56126 Pisa, Italy
(Received 1 November 1994; revised manuscript received 27 February 1995)

We solve the problem of the scattering of an electromagnetic plane wave from a planar array of equispaced cylindrical scatterers with strong resonances. We apply this theory to calculate the reflectivity of an array of quantum wires using the electromagnetic properties of the single wire as the only input. We find electromagnetic interference between the wires, whose effects are additional shifts and broadenings of the isolated wire resonances. A detailed analysis of some commonly used experimental configurations is also presented, with evidence of interference effects. Resonance shifts and broadenings are also interpreted as properties of the mixed modes of the quantized electromagnetic fields and the full grating excitations, i.e., grating polaritons. Stationary modes of the grating polaritons are also found, which have the peculiar property of being guidedlike modes sustained by electronic excitations confined along one propagation direction.

I. INTRODUCTION

Semiconductor structures where the electronic excitations are confined in two directions and propagating as one-dimensional modes are today produced with the use of advanced nanofabrication techniques.[1] Thus many properties of one-dimensional excitations can now be experimentally investigated. In particular, the optical properties also give information on their interaction with light. However, these wire structures are usually produced in an array configuration, which we call a quantum grating (QG):[1,2] although the existence of thick potential barriers for the electronic excitations between the wires ensures that they remain one dimensional, we expect the optical response of the system to be influenced by the mutual interwire electromagnetic interference. It is therefore necessary to calculate the optical response of the *full* grating structure. In this way we may establish a relationship between the optical properties of the grating and the electronic properties of the single wires.

D'Andrea and Del Sole[3] calculated the optical response (reflectivity and absorption) of these grating structures. They considered wires with a rectangular section, where the exciton confinement is incomplete in the larger dimension. This rectangular shape is typical of wires obtained from etched quantum-well structures.[4,2] In this calculation, the effects of grating electromagnetic interference, although implicitly included, are not evident since the starting point is the *full* grating as the optically active material.

In this paper we study the electromagnetic properties of the QG using the *optical* properties of a *single* wire as the basic building block. The optical response of the full grating is then obtained by considering the waves multiply scattered from the single wires. This approach naturally allows us to isolate the effects of the interference between the wires and to recover the true energies of the electronic excitations from the reflectivity spectra of the full grating. The results of our theory and those of D'Andrea and Del Sole are not directly comparable since we consider a simple model of a cylindrical wire in place of the more elaborate model of the asymmetrical wire with rectangular section. Our theory disregards these aspects of real wires, but rather focuses on the changes of the optical properties in passing from the single wire to the grating configuration. It is, however, fair to notice that improvements in lithographic technology today allow full one-dimensional confinement to be achieved,[1,2] which shows the practical relevance of our approach. In principle, it would also be possible to consider cases of lower symmetry for the wire arrangements, but analytic results would not obtain in general.

In this work we also examine the connection between the calculated optical response and the quantized electromagnetic modes of the full grating structure. These two approaches turn out to be complementary for the understanding of the physical aspects of the optical properties of the grating structures, as pointed out by Citrin[5] for the multi-quantum-well (MQW) case. In the first approach a superposition of scattered partial waves of isolated structures is considered and the effects of multiple scattering on the global grating response is put into evidence. Strong wire interference is expected when the interwire spacing is smaller than the wavelength of light. In the second approach the transition towards the two-dimensional behavior of the excitation due to inter-

0163-1829/95/51(23)/16973(11)/$06.00

wire interference naturally comes out from the study of the imaginary part of the exciton propagator (polariton radiative broadening), which shows a typical two-dimensional behavior when the electromagnetic coupling between the wires becomes strong. Finally, the polariton approach predicts most naturally the existence of stationary modes, which are waveguidelike but sustained by electronic excitations that are in fact localized along one of the propagation directions. This type of polariton therefore shows some analogies to Frenkel exciton polaritons of organic quantum wells (QW's), along one propagation direction (see, for example, the superradiant properties of these materials reviewed by Agranovich in Ref. 6).

The article is subdivided as follows. In Sec. II we briefly introduce the electromagnetic modes associated with a cylindrical wire and the scattering coefficients for the optically active ones. In Sec. III we formulate a theory of the response of the grating to an incoming electromagnetic plane wave. Analytic formulas for the reflectivity at any angle of incidence and polarization are given and the effect of wire interference is thoroughly analyzed in specific experimental configurations. Numerical examples in the previous configurations, with parameters chosen close to those of real GaAs structures, are presented in Sec. IV. They give evidence for measurable interference effects, which consist of shifts of the reflectivity peak positions and changes in oscillator strengths with the incidence angle and/or polarization. In Sec. V we propose a qualitative model for the elementary excitations of the QG and give their interpretation in terms of two-dimensional Wannier-Frenkel polaritons of the full grating. Surface modes appear as a natural extension of those that are instead involved in the reflectivity. The existence of surface grating modes at the exciton energy for wires spaced less than the wavelength of light is also remarked. A discussion and conclusions are finally given in Sec. VI.

II. QUANTUM WIRE ELECTROMAGNETIC MODES

In this section we briefly describe how the close-to-resonance optical properties of a cylindrical wire can be represented. A free electromagnetic field in the barrier region, i.e., outside the wire, can be described as a suitable superposition of incoming and outgoing waves of cylindrical symmetry, $\mathbf{E}_{\mathrm{inc},m,i}$ and $\mathbf{E}_{\mathrm{out},m,i}$, respectively, centered on the wire axis:

$$\mathbf{E}=\sum_{m,i}\epsilon_{\mathrm{inc},m,i}\mathbf{E}_{\mathrm{inc},m,i}+\epsilon_{\mathrm{out},m,i}\mathbf{E}_{\mathrm{out},m,i}. \tag{1}$$

These modes of the barrier of cylindrical symmetry are labeled by a translational quantum number $k_{\|}$, an azimuthal integer m, and a polarization index i. The modes having $m\neq 0$ are not fully transverse, but two hybrid modes HE and EH are found.[7] In a cylindrical coordinate system having directions $\hat{x},\hat{\rho},\hat{\phi}$, $\hat{x}$ being along the wire axis, the electric field components are

$$\begin{aligned}&E_\rho+iE_\phi=\tfrac{k}{k_0}H_{m+1}(k\rho),\\&E_\rho-iE_\phi=\tfrac{k_+^2}{k\,k_0}H_{m-1}(k\rho),\\&E_x=\tfrac{k_\|}{ik_0}H_m(k\rho);\end{aligned}$$

$$\begin{aligned}&E_\rho=-\tfrac{ik_\|}{k}H_{m+1}(k\rho),\\&E_\phi=-iE_\rho,\\&E_x=H_m(k\rho)\end{aligned} \tag{2}$$

for the HE and the EH modes, respectively. Here H_m is a Hankel function of order m of the first (second) kind,[8] for the incoming (outgoing) wave, and $k_0^2=\omega^2/v^2$, $k^2=k_0^2-k_\|^2$, $k_+^2=k_0^2+k_\|^2$, and v is the velocity of light in the medium. For $m=0$, it is possible to take a suitable combination of the modes (2) to obtain TE and TM modes, respectively,

$$\begin{aligned}&E_\rho=0,\quad E_x=0,\quad E_\phi=H_1(k\rho);\\&E_\phi=0,\quad E_\rho=-\frac{ik_\|}{k}H_1(k\rho),\quad E_x=H_0(k\rho).\end{aligned} \tag{3}$$

The incoming and the outgoing waves introduced in Eq. (1) are not independent since the scatterer converts incoming waves into outgoing waves. This means that the properties of the scatterer define the ratios between ϵ_{inc} and ϵ_{out} in Eq. (1), i.e., a scattering coefficient α:

$$\alpha_{m,i}=\frac{\epsilon_{\mathrm{out},m,i}}{\epsilon_{\mathrm{inc},m,i}}. \tag{4}$$

We notice that in the scattering, the wave numbers $k_{\|}$ and m are conserved due to the symmetry of the problem. Thus the high symmetry of the system allows a simple description of the scattering properties of the modes. Useful guidelines for the comprehension of systems of lower symmetry are, however, obtained. The scattering coefficients of cylindrical wires containing one-dimensional excitons have been calculated in Ref. 9. They were obtained by solving Maxwell equations with the microscopically calculated nonlocal exciton susceptibility:

$$\chi(\boldsymbol{\rho},\boldsymbol{\rho}')=\frac{i}{\hbar}\sum_{\mathrm{ex}}\left[\frac{\boldsymbol{\mu}_{cv}\otimes\boldsymbol{\mu}_{cv}}{\omega_{\mathrm{ex}}-\omega-i\epsilon}\right]f_{\mathrm{ex}}(\boldsymbol{\rho})f_{\mathrm{ex}}(\boldsymbol{\rho}')|F_{\mathrm{ex}}(0)|^2, \tag{5}$$

where $f_{\mathrm{ex}}(\boldsymbol{\rho})$ is the exciton confinement function, given by the product of the electron and the hole confinement wave functions, $F_{\mathrm{ex}}(x)$ is its envelope wave function, $\hbar\omega_{\mathrm{ex}}$ is its energy, and $\boldsymbol{\mu}_{cv}$ is the dipole matrix element between the valence and the conduction bands. The polarization reads

$$\mathbf{P}(\boldsymbol{\rho})=\int d\boldsymbol{\rho}'\chi(\boldsymbol{\rho},\boldsymbol{\rho}')\mathbf{E}(\boldsymbol{\rho}'). \tag{6}$$

Notice that it is evidently confined inside the wire by the first $f_{\mathrm{ex}}(\boldsymbol{\rho})$ factor in $\chi(\boldsymbol{\rho},\boldsymbol{\rho}')$ [Eq. (5)] and it is proportional to the integral of the electric field with the exciton confinement function through the other $f_{\mathrm{ex}}(\boldsymbol{\rho}')$. The susceptibility Eq. (5) is calculated within a two-band effective mass model for the semiconductor band edge. For the lowest energy exciton, which is the only one included in the susceptibility, the envelope function has full

azimuthal symmetry. Only cylindrical waves that have at least an azimuthally constant electric field component produce a polarization of the wire and a scattering of the incoming wave. These modes, which we call active, are either L modes with TM character, which develop a polarization along the wire axis, or wire (W) modes with $m = \pm 1$ and HE character, which instead have a polarization orthogonal to the wire axis.[9] Because of the cylindrical symmetry, these latter two modes are degenerate. This degeneracy is removed in real samples by the anisotropy of the confining potential, so that in a QG structure we may expect two modes of different energy, one with polarization into the grating plane, the other orthogonal to it.

When the fourfold degeneracy of the valence band of III-V semiconductors at the Γ point is considered, the exciton wave function $f_{\rm ex}(\boldsymbol{\rho})$ and the dipole matrix element $\boldsymbol{\mu}_{cv}$ become multicomponent. In order to build the former functions, the electron and the hole subbands for the confined cylindrical geometry first have to be calculated in the full multiband effective mass theory. These subband wave functions have been derived exactly by Sercel and Vahala[10] in a basis of cylindrical coordinates. They are labeled by an azimuthal quantum number F_z and the lowest (doubly degenerate) electron and hole subbands have $F_z = \pm 1/2$. Four excitons of different azimuthal symmetry are thus found and they are degenerate provided the exchange splittings are neglected. They all contribute with the same energy $\hbar\omega_{\rm ex}$ to the susceptibility Eq. (5), which in the multiband case also contains a summation on the different band contributions. The active modes of the electromagnetic field are those that produce a nonvanishing polarization integral. In particular, the azimuthal integration has to be nonvanishing. This shows that all six $m = 0$ and ± 1 modes given in Eqs. (2) and (3) are optically active, while all the others are optically inactive.

However, other approximate selection rules produced by the radial integration in the polarization integral hold. In fact, the exciton envelope function is confined in a region of the size of the wire radius R. An electric field component that is proportional to a Bessel function of order n produces a radial integral proportional to $(R/\lambda)^n$, where λ is the wavelength of light. Since $\lambda \gg R$, not all of the six modes considered before are in practice optically active, but only those that have an $n = 0$ component. In particular, for m=0 only the TM mode is active and it turns out to have polarization along x. For $m = \pm 1$ only one of the two HE and EH modes is practically active and has polarization in the plane perpendicular to the wire axis. The first mode again is an L mode and the other two modes are again degenerate W modes. The same active modes as in the simpler two-band model are therefore found. We conclude that when the correct multiband approach to the exciton and therefore to the susceptibility of the cylindrical wire is used, the results of Ref. 9 are not modified on a qualitative level. Only the ratio between the oscillator strengths of the L and the W modes may become different from the one assumed. This ratio is in fact fixed by the symmetry of the electron and the hole subbands considered, in analogy to what happens in the case of the QW for the ratio of the in-plane and the off-plane oscillator strengths.

The resonant-type response of the exciton in the susceptibility produces a Breit-Wigner resonance in the scattering coefficients of the optically active modes. Optically inactive modes instead have a trivial scattering coefficient, which can be taken to be unity.

The two W modes are associated with the same scattering coefficient

$$\alpha_W = \frac{\omega - \omega_W + i\Gamma_W - i\gamma}{\omega - \omega_W - i\Gamma_W - i\gamma}. \tag{7}$$

An analogous Breit-Wigner expression holds for α_L. Here ω_W and (ω_L) are the resonance frequencies of the W and the L mode, respectively, and Γ_W and Γ_L their related radiative broadening. A phenomenological broadening γ has also been added to take into account the homogeneous broadening of the resonances. We give here simplified expressions for the L-W splitting and the broadenings and refer to Ref. 9 for a complete derivation:

$$\omega_W - \omega_L \simeq \frac{1.6 \times 10^6}{\epsilon_\infty R(\text{Å})^2}\, \Gamma_0(R), \tag{8}$$

$$\Gamma_W \simeq \frac{k_0^2 + k_\parallel^2}{2k_0^2}\, \Gamma_0(R),$$

$$\Gamma_L \simeq \frac{k_0^2 - k_\parallel^2}{k_0^2}\, \Gamma_0(R), \tag{9}$$

where $\Gamma_0(R)$ is proportional to the oscillator strength of the one-dimensional wire exciton only, R being the wire radius

$$\Gamma_0(R) \simeq \frac{\pi \mu_{cv}^2 |F_{\rm ex}(0)|^2 k_0^2}{\epsilon_\infty}. \tag{10}$$

Here ϵ_∞ is the index of refraction of the barrier material.

III. SOLUTION OF THE GLOBAL SCATTERING PROBLEM

A. Formulation of the problem for the general case

We have explained how the full description of the electromagnetic properties of the quantum-well wire (QWW) is given by the scattering coefficients introduced in the preceding section. We now consider an incoming plane wave on the grating, whose propagation direction can be defined using two different incidence angles, as shown in the geometry of the ideal experiment in Fig. 1. In order to understand how the incoming plane wave is scattered by the grating, it is convenient to introduce the concept of scattered wave. Quite generally, for any scattering experiment, we may define the scattered waves as the difference of the outgoing waves with and without the scatterer. Therefore, a scattered wave exists only in the case that the scattering coefficient associated with it is nontrivial. For an isolated wire, the scattered field is given by

$$\mathbf{E}_{\rm scatt}(\mathbf{r}) = \sum_m (\alpha_m - 1)\, \epsilon_{{\rm inc},m} \mathbf{E}_{{\rm out},m}(\mathbf{r}), \tag{11}$$

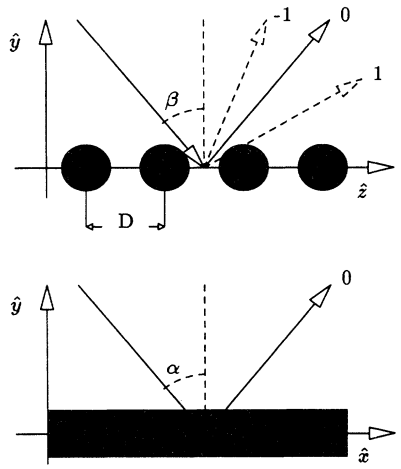

FIG. 1. Example of geometrical configuration of light diffraction experiment for a QG. On the top, a section orthogonal to the wire (black circles) axes is shown. The conventional choice of axes are indicated. The incident and the reflected directions are indicated by solid arrows. Higher orders of grating diffraction are indicated as dashed arrows. The incidence angle in this direction is also indicated. On the bottom, a section parallel to the wire axis (black rectangles) is shown. The relationship between the incidence angle and the components of the incident wave vector $\mathbf{k}_0 = (k_x, k_y, k_z)$ is given by $\sin(\beta) = k_z/k$, $\sin(\alpha) = k_x/\sqrt{k_0^2 - k_z^2}$, and $k_{\|} = k_x$.

where the outgoing type fields were introduced in the preceding section. When we consider the full grating, the scattered electric field is built up from the superposition of the scattered fields of each wire

$$\mathbf{E}_{\mathrm{scatt}}(\mathbf{r}) = \sum_n \mathbf{E}^{(n)}_{\mathrm{scatt}}(\mathbf{r}), \tag{12}$$

where $\mathbf{E}^{(n)}_{\mathrm{scatt}}(\mathbf{r})$ is the scattered field of the nth wire. In order to calculate the scattered fields of the single wires, using Eq. (11), we need to know the coefficients $\epsilon_{\mathrm{inc},m}$ that are used in it. Now let us consider a given fixed wire n. As we remarked at the beginning of Sec. II, any field around it may be divided into incoming and outgoing components. Therefore, also the incoming plane wave and all the scattered fields of the other wires produce incoming waves on it. We may therefore write

$$\epsilon^{(n)}_{\mathrm{inc},m} = \epsilon^{\mathrm{source}}_{\mathrm{inc},m}\, e^{in\phi_0} + \sum_{\substack{n' \neq n \\ m'}} \mathcal{S}^{n-n'}_{mm'} \epsilon^{(n')}_{\mathrm{scatt},m'} \tag{13}$$

where $\epsilon^{(n')}_{\mathrm{scatt},m'} = (\alpha_{m'} - 1)\epsilon^{(n')}_{\mathrm{inc},m'}$ and $\phi_0 = k_z D$ is the phase difference of the incoming plane wave between adjacent wires spaced by D. The quantity $\mathcal{S}^{n-n'}_{mm'}$ is a projection coefficient that gives the incoming wave (of type m) on wire n produced by the scattered wave (of type m') generated at wire n'; its expression is given in the Appendix. The coefficients $\epsilon^{\mathrm{source}}_{\mathrm{inc},m}$ give instead the decomposition of the incoming plane wave into incoming components of cylindrical symmetry.

The quantities $\epsilon^{(n)}_{\mathrm{inc},m}$ are found by solving Eq. (13). This system of equation is easily solved with respect to the index n by using the translational symmetry of the problem

$$\epsilon^{(n)}_{\mathrm{inc},m} = \epsilon^{(n-1)}_{\mathrm{inc},m}\, e^{i\phi_0}. \tag{14}$$

Equation (13) then reduces to

$$\sum_{m'} \left[\delta_{mm'} - (\alpha_{m'} - 1) \sum_{n \neq 0} \mathcal{S}^{n}_{mm'} e^{in\phi_0} \right] \epsilon^{(0)}_{\mathrm{inc},m'} = \epsilon^{\mathrm{source}}_{\mathrm{inc},m}. \tag{15}$$

We further observe that only for a few m' we have an active mode, i.e., $\alpha_{m'} \neq 1$. For these active modes, Eq. (13) reduces to a finite system of linear equations,[11] which can be easily solved. The scattered field in Eq. (12) can thus finally be calculated.

Let us now consider the problem of extracting the various orders of grating diffraction from the total scattered field. This field has the same translational property of the incoming wave coefficients [Eq. (14)] since both originate from the translational symmetry of the problem

$$\mathbf{E}_{\mathrm{scatt}}(\mathbf{x} + n\hat{z}D) = e^{in\phi_0}\mathbf{E}_{\mathrm{scatt}}(\mathbf{x}). \tag{16}$$

This translational property suggests the following Fourier representation of the scattered field:

$$\mathbf{E}_{\mathrm{scatt}}(\mathbf{x}) = e^{ik_{\|}x} \sum_l \left[\mathbf{c}_{l,\mathrm{inc}}(k_{\|}, k_0) e^{-ik_y^{(l)} y} + \mathbf{c}_{l,\mathrm{out}}(k_{\|}, k_0) e^{ik_y^{(l)} y} \right] e^{i(k_z + \frac{2\pi}{D} l)z}, \tag{17}$$

where l is an integer,

$$k_y^{(l)\,2} = k^2 - \left(k_z + \frac{2\pi}{D} l\right)^2,$$

and we have to take $\mathrm{Im}(k_y) > 0$ when $y > 0$ and $\mathrm{Im}(k_y) < 0$ when $y < 0$. It is now clear that the Fourier components of the expansion given in Eq. (17) represent the various orders of grating diffraction. These Fourier components may be easily calculated. In particular, for the reflectivity of order zero we have

$$\begin{aligned} \mathbf{c}_{0,\mathrm{out}} e^{ik_y^{(0)} y_0} &= \frac{1}{D} \int_0^D dz\; e^{-ik_z z} \mathbf{E}_{\mathrm{scatt}}(y_0, z) \\ &= \sum_m \frac{1}{D} (\alpha_m - 1) \\ &\quad \times \int_{-\infty}^{+\infty} dz\; e^{-ik_z z} \epsilon^{(0)}_{\mathrm{inc},m} \mathbf{E}^{(0)}_{\mathrm{out},m}(y_0, z). \end{aligned} \tag{18}$$

Other orders of diffraction are similarly found.

B. Solutions for the general case

We analytically solve all the equations given in the preceding steps in order to provide analytic formulas for the reflectivity of the quantum grating for a generic experimental configuration, i.e., for generic angles of incidence and polarizations. The system of equations (15) for the active modes is rewritten by introducing the Σ_{ij} functions:

$$\epsilon^i_{\rm inc} - \sum_j \Sigma_{ij}(\alpha_j - 1)\epsilon^j_{\rm inc} = \epsilon^{i,\rm source}_{\rm inc}, \tag{19}$$

where $i,j = W_{-1}, L, W_1$ labels the three optically active modes of the wires. The Σ functions are defined from the $\mathcal{S}$ projection coefficients calculated in the Appendix and are given by

$$\Sigma_{W_1W_1} = \Sigma_{W_{-1}W_{-1}} = \Sigma_{LL} = \Sigma_0,$$

$$\Sigma_{W_1W_{-1}} = \Sigma_{W_{-1}W_1} = \frac{k^2}{k_+^2}\Sigma_2,$$

$$\Sigma_{W_1L} = -\Sigma_{LW_1} = -\Sigma_{W_{-1}L} = \Sigma_{LW_{-1}} = \frac{ik_0k_\parallel}{k_+^2}\Sigma_1,$$

where (20)

$$\Sigma_m(k_z,kD) = \frac{1}{2}\sum_{n\neq 0} e^{ik_zD\,n}H_m(|n|kD). \tag{21}$$

The incoming source field components appearing in Eq. (19) are the following functions of the unitary polarization vector $\hat{\varepsilon}$:

$$\epsilon^{W_1,\rm source}_{\rm inc} = \frac{k^2}{k_+^2}\left[\frac{k}{2k_0}\varepsilon_{z+iy} + \frac{k_+^2}{2kk_0}\varepsilon_{z-iy}e^{-i2\beta} - \frac{k_\parallel}{ik_0}\varepsilon_x e^{-i\beta}\right] = \epsilon^{W_{-1},\rm source*}_{\rm inc}, \tag{22}$$

$$\epsilon^{L,\rm source}_{\rm inc} = \frac{k^2}{k_+^2}\left[\frac{ik_\parallel}{2k}(\varepsilon_{z+iy}e^{-i\beta} - \varepsilon_{z-iy}e^{i\beta}) + \varepsilon_x\right], \tag{23}$$

where β is the incidence angle in the y-z plane, $\sin(\beta) = k_z/k$. These function are simply calculated by decomposing a plane wave of polarization $\hat{\varepsilon}$ and wave vector $\mathbf{k}$ into the cylindrical waves introduced in Sec. II.

Given the $\mathbf{k}$ and the $\hat{\varepsilon}$ vectors, fixed by the experimental configuration, the incoming components for the active modes are calculated using Eq. (19) and the scattered field is calculated using Eq. (11). Finally, we integrate the various components of the cylindrical fields as in Eq. (18). This can be easily done using a few identities for the integration of the Hankel functions, obtained in the Appendix. Here we write the result for the three Cartesian components of the reflected field:

$$E_x = \frac{2e^{ik_yy}}{k_yD}\left[\frac{k_\parallel}{ik_0}(\alpha_W - 1)\left(e^{-i\beta}\epsilon^{W_1}_{\rm inc} - e^{i\beta}\epsilon^{W_{-1}}_{\rm inc}\right) + (\alpha_L - 1)\epsilon^L_{\rm inc}\right], \tag{24}$$

$$E_y = \frac{e^{ik_yy}}{k_yD}\left[\frac{(\alpha_W - 1)}{ikk_0}[(k^2e^{-i2\beta} - k_+^2)\epsilon^{W_1}_{\rm inc} - (k^2e^{i2\beta} - k_+^2)\epsilon^{W_{-1}}_{\rm inc}] - 2(\alpha_L - 1)\frac{k_\parallel}{k}\cos(\beta)\epsilon^L_{\rm inc}\right], \tag{25}$$

$$E_z = \frac{e^{ik_yy}}{k_yD}\left[\frac{(\alpha_W - 1)}{kk_0}[(k^2e^{-i2\beta} + k_+^2)\epsilon^{W_1}_{\rm inc} + (k^2e^{i2\beta} + k_+^2)\epsilon^{W_{-1}}_{\rm inc}] - 2(\alpha_L - 1)\frac{k_\parallel}{k}\sin(\beta)\epsilon^L_{\rm inc}\right]. \tag{26}$$

Both the reflectivity modulus and the polarizations can be calculated from the above field components for any angle of incidence and polarization of the incoming plane wave. The same procedure, i.e., the extraction of Fourier components from the scattered field, could be used for the other orders of grating diffraction.

IV. GRATING REFLECTIVITY FOR SPECIFIC CASES

We consider two specific reflectivity experiments that are commonly carried out on the grating structures. In the first type of experiment, the plane of incidence is orthogonal to the wire axis, case O, and the angle of incidence is varied within this configuration. The polarization may be either orthogonal to the plane of incidence (case Os) or parallel to it (case Op). In the second type of experiment, the plane of incidence is perpendicular to the grating, but parallel to the wire axis (case P). Also in this case we may have orthogonal (Ps) or parallel (Pp) polarizations of the incident plane wave. In the O configuration we have $k_\parallel = 0$, but, at an angle of incidence, $k_z \neq 0$. In the P configuration we have $k_z = 0$ and usually $k_\parallel \neq 0$.

Let us show explicitly the reflectivity of the Os configuration. In this case the electric field is along the wire axis and therefore only the L mode is excited. From Eqs. (24)–(26), using a polarization vector $\hat{\varepsilon}_s = (1,0,0)$, we obtain the result that the reflected wave is also s polarized, in agreement with the symmetry of the problem. The reflectivity is

$$r_{\rm Os} = \frac{\alpha_L - 1}{k_yD}\frac{2}{1 - (\alpha_L - 1)\Sigma_0(k_z)}, \tag{27}$$

where we have discarded superflous phase factors. We recall that $k_y^2 = k^2 - k_z^2$. It is clear that interference effects between the wires are contained in the denominator of Eq. (27). If we now substitute α_L from Eq. (7) into (27) we obtain

$$r_{\rm Os} = \frac{4i\Gamma_L}{k_yD}\frac{1}{\omega - \omega_L - i\Gamma_L[1 + 2\Sigma_0(k_z)] - i\gamma}. \tag{28}$$

We can see that $|r_{\rm Os}|^2$ has the simple shape of a resonance. However, the resonant frequency is shifted from

the L mode eigenfrequency ω_L due to the the imaginary part of Σ_0. This is clearly an effect of the electromagnetic interference between the wires. The real part of Σ_0 in the denominator increases instead the radiative broadening of the resonance Γ_L. This broadening is also divided by k_yD in the numerator. Both effects amount to a change of the oscillator strength of the resonance. If we calculate the strength of the reflectivity peak by integrating $|r_{Os}|^2$ over the frequency, we obtain

$$\frac{16\Gamma_L^2}{(k_yD)^2\{\Gamma_L[1+2\mathrm{Re}(\Sigma_0)]+\gamma\}}. \tag{29}$$

Now $2\pi/(k_yD)$ is the number of wires seen by the incoming plane wave inside a wavelength. This means that the wires inside this length emit almost coherently, so that their emission becomes coherently added in the reflectivity. The Σ_0 correction in the denominator is instead a multiple interference effect. It is interesting to notice that, as we go to grazing incidence, $k_y \to 0$, but also $\mathrm{Re}(\Sigma_0) \simeq (k_yD)^{-1}$, so that a true two-dimensional limit is recovered, where the radiative broadening and therefore the strength of the resonance increases as $(k_yD)^{-1}$.[12] In other words, the system responds as if the material excitation were bidimensional, although the electronic excitations are one dimensional.

We report in Fig. 2 both the real and the imaginary parts of Σ_0 as functions of k_z, for an interwire spacing corresponding to $kD = 0.25$. We may read from this figure the shift of the peak of the reflectivity as a function of the incidence angle by scaling the imaginary part of Σ_0 with Γ_0. Since typical values of Γ_0 for GaAs wires

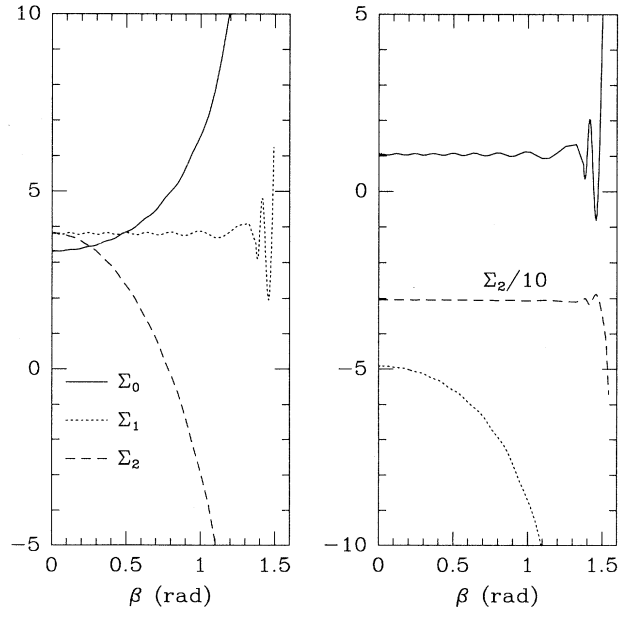

FIG. 2. Real (solid) and imaginary (dashed) parts of Σ_0 at $k_\parallel = 0$, as functions of β. The Σ_i were introduced in Eq. (21).

amount to a few tens of μeV, small shifts of the order of tenths of meV are expected for reasonable wire separations.

In the Op case, the electric field is orthogonal to the wire axis and the two W modes are excited. In this case, always using Eqs. (24)–(26), with a polarization vector $\hat{\varepsilon}_p = (0, k_z/k_0, -k_y/k_0)$ for the incident plane wave, we obtain

$$r_{\mathrm{Op}} = \frac{2(\alpha_W-1)}{k_yD}\left(\frac{\sin^2(\beta)}{1-(\alpha_W-1)(\Sigma_0-\Sigma_2)} + \frac{\cos^2(\beta)}{1-(\alpha_W-1)(\Sigma_0+\Sigma_2)}\right), \tag{30}$$

where all the symbols have been previously introduced. At an angle of incidence, the degeneracy of the two W modes is removed, i.e., two different resonant energies are found. The symmetry lowering of the system in this reflectivity configuration is of course produced by the interference between the wires. As in the Os case, these are additional shifts and additional broadenings of the resonance peaks, which also produce a variation of their relative heights and strengths. In real samples, we must recall that the degeneracy of the W modes is already removed at the level of the exciton energies because of the wire asymmetry. For rectangular wire sections, we may expect two types of excitons having z and y directed optical dipols. The z directed dipole is therefore excited at normal incidence ($\beta = 0$ and $k_z = 0$), while the other is excited at grazing incidence. In this realistic case, the shifts produced by the interference between the wires mix with those produced by the wire asymmetry. It is, however, useful to deduce the shift of the reflectivity peak between normal and grazing incidence produced by wire interference only. From Eq. (30) we see that it can be analytically written as

$$\Delta\omega_{\mathrm{O}} = 2\ \mathrm{Im}(\Sigma_2)\Gamma_0, \tag{31}$$

where $\mathrm{Im}(\Sigma_2)$ can be evaluated at normal incidence, since its value is fairly independent of the incidence angle in a broad range.

We report in Fig. 3 a set of two typical reflectivity curves obtained for the Os and the Op cases at almost normal and almost grazing incidence, respectively. Parameters were chosen close to those of a real GaAs-type quantum wire. A splitting of 1 meV between the L and the W mode was assumed and also $\Gamma_0 = 10$ μeV and $\gamma = 1.6$ meV. For the separation of the wires we used $kD = 0.25$, corresponding to a wire separation of about 200 nm, a typical value for currently grown structures, with wires separated by air.[4] We notice that from Eq. (31) a shift of 0.6 meV is expected, as indeed visible in the reflectivity spectra of Fig. 3. Recently, even closer packed structures have been realized, with interwire spacings as small as 32 nm for a GaAs buried QWW (see Gershoni *et al.* in Ref. 1). In this case we have $kD \simeq 0.1$ considering the wavelength of light in the material and therefore even larger energy shifts.

In the P case, both in s polarization and p polarization, the W modes remain degenerate because of the specular

symmetry with respect to the plane of incidence. In the Ps case, the mode L is not excited, while in the Pp case both W and L modes are. We give the full formulas for the reflectivity in these cases, neglecting superflous phase factors:

$$r_{\mathrm{Ps}} = \frac{k_0^2}{kDk_+^2} \frac{(\alpha_W - 1)}{1 - (\alpha_W - 1)\left(\Sigma_0 + \frac{k^2}{k_+^2}\Sigma_2\right)}, \tag{32}$$

$$r_{\mathrm{Pp}} = \frac{k_0^2}{kDk_+^2 \mathcal{D}} \left[(\alpha_L - 1)\mathcal{A}_W + 2\frac{k_\parallel^2}{k_+^2}(\alpha_W - 1)\mathcal{A}_L \right.$$

$$\left. + 4(\alpha_W - 1)(\alpha_L - 1)\frac{k_\parallel^2}{k_0^2}\Sigma_1 \right], \tag{33}$$

where we have used

$$\mathcal{D} = \mathcal{A}_L\mathcal{A}_W - 2\frac{k_\parallel^2 k_0^2}{k_+^4}\Sigma_1^2(\alpha_W - 1)(\alpha_L - 1)$$

and

$$\mathcal{A}_L = 1 - (\alpha_L - 1)\Sigma_0,$$

$$\mathcal{A}_W = 1 - (\alpha_W - 1)\left(\Sigma_0 - \frac{k^2}{k_+^2}\Sigma_2\right).$$

We notice that in p polarization, the W and the L modes become separated if

$$\left|\Sigma_1^2(\alpha_W - 1)(\alpha_L - 1)\right| \ll 1,$$

or equivalently if

$$\Gamma_0|\Sigma_1(kD)|/\Delta\omega_{WL} \ll 1. \tag{34}$$

In this case the L and the W resonances contributing to the p reflectivity are well separated, and the Pp reflectivity curve is given by two independent resonances corresponding to the L and W modes:

$$r_{\mathrm{Pp}} \simeq \frac{k_0^2}{kDk_+^2}\left[\frac{(\alpha_L - 1)}{1 - (\alpha_L - 1)\Sigma_0} \right.$$

$$\left. + 2\frac{k_\parallel^2}{k_0^2}\frac{(\alpha_W - 1)}{1 - (\alpha_W - 1)\left(\Sigma_0 - \frac{k^2}{k_+^2}\Sigma_2\right)} \right]. \tag{35}$$

However, shifts and broadenings caused by the interference between the wires also appear as in the other cases. These shifts and broadenings are again related to the imaginary and the real parts of the Σ_0 and the Σ_2 functions, as seen in detail for the case Os. In the opposite case of relevant mixing between the L and the W modes, i.e., when the approximation (34) does not apply, a gain of strength of one peak at the expenses of the other would be found, with additional shifts of their positions.

We plot $\Sigma_0, \Sigma_1, \Sigma_2$ in Fig. 4 as functions of kD at $k_z = 0$. We notice the divergence of these functions when $kD \to 0$, similar to the one found at grazing incidence in the O case. This is related to the recovery of the

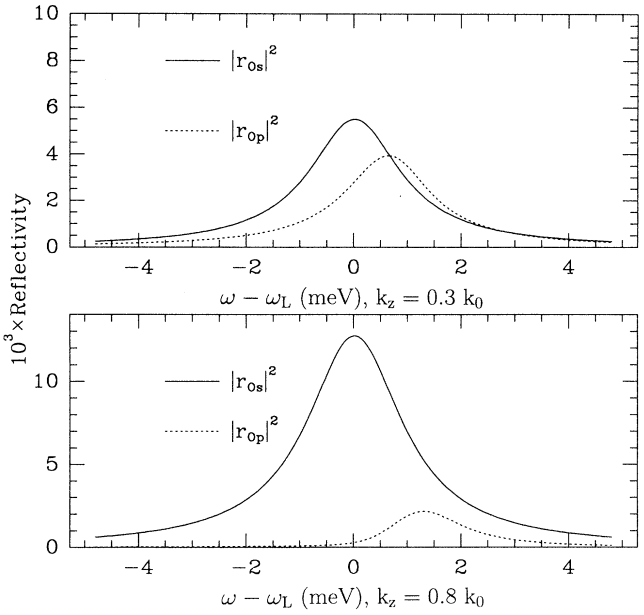

FIG. 3. Two typical reflectivity curves in the O configuration (see the text) at two different incidence angles; the first is at almost normal incidence, the second at almost grazing incidence. The parameters used in the calculation are given in the text. The center of mass dispersion of the exciton was not included in the calculation for clarity.

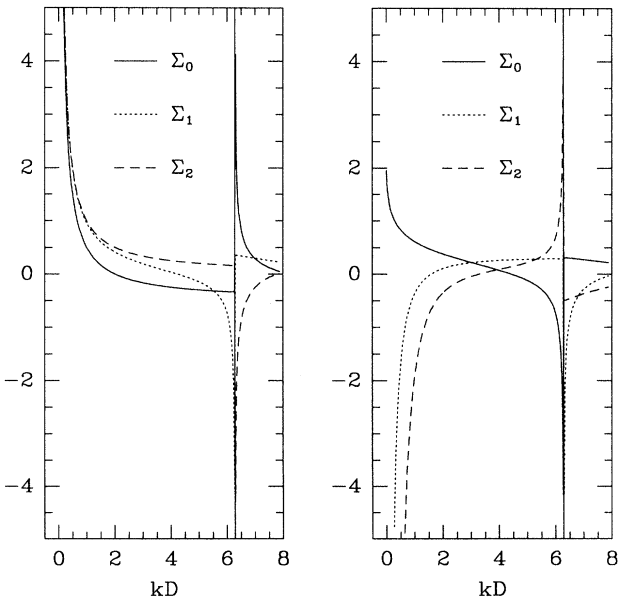

FIG. 4. Real (on the left) and imaginary (on the right) parts of the Σ_0, Σ_1, and Σ_2 coefficients introduced in Eq. (21), as functions of kD, at $k_z = 0$.

two-dimensional limit at grazing incidence as discussed in the Os case. We may notice from this figure that $k|\Sigma_1|$ slowly diverges at small k and roughly as D^{-1} at small D, so that we may expect relevant L-W mixing for some closely packed gratings close to grazing incidence. However, in real GaAs samples, with oscillator strengths of the order of magnitude given in the example before, these conditions are not practically accessible for any wire spacing and/or incidence angle. The possibility of observing such effects in other materials that have larger oscillator strengths but smaller W-L splittings remains to be investigated. A comparison should also be made with the MQW calculations of Andreani[13] and Citrin.[5] In the MQW case, an analogous L-Z mixing in p polarized modes is expected because of the reduction of the symmetry when passing from the single to the MQW case. Citrin has shown that this L-Z mixing is negligible in most of the radiative region where $k_{\|} < k_0$. A crossover region where the mixing is not negligible certainly exists, as shown by Andreani in his polariton dispersion curves for p polarization. An L-Z polariton crossover is in fact found across the photon dispersion at $k_{\|} \neq 0$. The actual experimental accessibility of this small dispersion region where the mixing effects could be observed remains to be clarified. In our QG case we have practically excluded any accessibility to such regions of the dispersion.

We show in Fig. 5 two typical reflectivity curves at two different angles of incidence for both s and p polarization, for the same QG structure used in the O case. A comparison of the shifts of the peak associated with the W modes in p and s polarizations at grazing incidence [Eqs. (32) and (35), respectively], shows that their difference is given by

$$\Delta\omega_{sp} = \frac{2k^2}{k_+^2} \operatorname{Im}(\Sigma_2)\Gamma_0. \tag{36}$$

Despite the divergence of the imaginary part of Σ_2 at small kD, this separation remains finite and is also rather flat in this region of small separations. It amounts to 0.6 meV in the case shown and could be observed as a shift of the reflectivity peak at grazing incidence when the polarization is appropriate. Such an experiment would be analogous to the one carried out on quantum wells to detect the depolarization shifts of the Z mode.[14] However, we must recall that a real sample shows strong anisotropies of the W exciton energies. These excitons are characterized by $\hat{z}$ or $\hat{y}$ polarizations as explained before and are thus preferentially excited in s and p polarization, respectively, at grazing incidence. As in the Op case, the interference shifts become entangled with those originated from the splitting of the wire modes.

Some interesting conclusions may, however, be made even for real structures. Though the interference shifts may not be practically resolved in the reflectivity spectra of actual samples, they may contribute to enlarge their "inhomogeneous" broadening by a sizable amount. Moreover, they also contribute to changing the radiative lifetimes. Similar conclusions have in fact been proposed for the MQW structures by Wang and Birman[15] and by Citrin[16] for double-well structures. It remains to be observed that inhomogeneities in the energies of different wires presumably wash out the interference effects previously found, at least when their magnitude becomes larger than the typical interference energies calculated here. Some detailed analysis is therefore needed to understand the influence of these inhomogeneities. This analysis may be carried out within the same approach presented here, although it is well understood that Eq. (13) should be solved numerically due to the lack of translational symmetry of such a nonhomogeneous case.

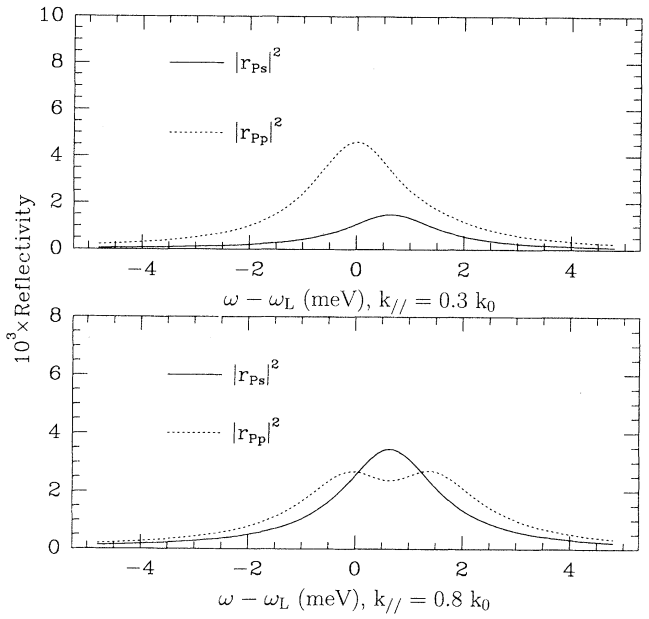

FIG. 5. Two typical reflectivity curves in the P configuration (see the text) at two different incidence angles; the first is at almost normal incidence, the second at almost grazing incidence. The parameters used in the calculation are given in the text. The center of mass dispersion of the exciton was not included in the calculation for clarity.

V. THE GRATING POLARITON

We now wish to consider the problem of the optical response of the grating structure from a different viewpoint, that of an array of one-dimensional excitons in a grating configuration, coupled to the electromagnetic field so as to build the electromagnetic modes of the grating structure. In optical experiments, it is these polariton modes of the whole structure that are excited. It is therefore interesting to study the connections of this approach with the previous one in the optical response that starts from the response of the single wire. This type of comparison is similar to the one carried out in detail by Citrin for the MQW case.[5] There a "material approach," in which the interacting propagators for the full MQW structure are calculated (and therefore the dispersion properties of the full-structure modes), is compared to an "optical ap-

proach," which uses the transfer matrix of the isolated wells to calculate the reflectivity and transmission of the MQW structure. It is shown that equivalent results are in fact obtained for radiative shifts and broadenings, but the material approach is more suitable for the calculation of spontaneous emission lifetimes, while the optical approach is more suited for the calculation of the optical response.

Citrin, in Ref. 17, considered the retarded electromagnetic coupling between grating excitons in the framework of this material approach. He simplified his model by neglecting the vectorial nature of the electromagnetic field and studied only the dispersion effects of the additional radiative shifts produced by the coupling. In this section we adopt the same model, but study instead only the effects on the radiative broadening. We do not discuss changes in frequency shifts since we know that they are rather dominated by the instantaneous response of the grating system (exchange effects), as already found also in the MQW systems by Wang and Birman.[15] These latter effects are clearly not contained in the material approach, which includes only the interaction with transverse electromagnetic fields. We know that these instantaneous effects are instead automatically included in the optical approach, also in the QG problem, and thus refer to Sec. IV for the complete results on the frequency shifts.

In our simplified model, the exciton destruction and creation operators are labeled by two indices only, a translational quantum number $k_x = k_{\|}$ and a wire index n, while the photon operators have the full translational quantum number $\mathbf{k}$. The Hamiltonian of the system, neglecting the A^2 term, which gives a negligible contribution near the exciton resonance, is

$$\mathcal{H} = \sum_{k_x,n} \hbar\omega_{k_x} b^\dagger_{k_x,n} b_{k_x,n} + \sum_{\mathbf{k}} \hbar c|\mathbf{k}| a^\dagger_{\mathbf{k}} a_{\mathbf{k}} + i \sum_{n,\mathbf{k}} C_{n,\mathbf{k}} (a^\dagger_{-\mathbf{k}} + a_{\mathbf{k}})(b^\dagger_{k_x,n} - b_{k_x,n}). \tag{37}$$

Here $\hbar\omega_{k_x}$ is the exciton energy, independent of n, and the interaction matrix element C is simply expressed in terms of the exciton and photon wave functions and the interaction $\mathbf{p}\cdot\mathbf{A}$ as

$$C_{n,\mathbf{k}} = \sqrt{\frac{2\pi}{\hbar c|\mathbf{k}| L_y L_z}}\, \omega_{k_x} \mu_{cv} F_{\mathrm{ex}}(0) \times e^{inDk_z} \int_{2D} d\boldsymbol{\rho}\, f_{\mathrm{ex}}(\boldsymbol{\rho}) e^{ik_y y + ik_z z} \tag{38}$$

where f_{ex} is the product of the confinement functions of the electrons and the holes, while F_{ex} is the envelope function. The momentum is conserved along the wire axis x in the interaction.

Excitons described in Eq. (37) have different character depending on the direction: they are Wannier excitons with respect to the wire axis, but in the z direction they are similar to molecular excitons without any possibility of hopping. They are also two dimensional, confined in the y direction. We may adopt a translational quantum number in the z direction, using a reduced Brillouin zone classification (i.e., $|k_z| < \pi/D$)

$$b_{k_x,k_z} = \frac{1}{\sqrt{N}} \sum_n e^{ink_zD}\, b_{k_x,n} \tag{39}$$

and an analogous one for $b^\dagger$. Here $N = L_z/D$ is the number of wires along z. It may be verified that the new operators indeed are bosons with normalized commutation relations if the $b_{k_x,n}$ also are. The Hamiltonian $\mathcal{H}$ in this representation becomes

$$\mathcal{H} = \sum_{k_x,k_z} \hbar\omega_{k_x} b^\dagger_{k_x,k_z} b_{k_x,k_z} + \sum_{\mathbf{k}_m} \hbar c|\mathbf{k}_m| a^\dagger_{\mathbf{k}_m} a_{\mathbf{k}_m} + i \sum_{\mathbf{k}_m} \sqrt{\frac{1}{DL_y}}\, \tilde{C}_{\mathbf{k}_m} (a^\dagger_{-\mathbf{k}_m} + a_{\mathbf{k}_m})(b^\dagger_{k_x,k_z} - b_{-k_x,-k_z}), \tag{40}$$

where the index m comes from the folding in the first Brillouin zone, $\mathbf{k}_m = (k_x, k_y, k_{z,m})$, $k_{z,m} = k_z + m2\pi/D$, and

$$\tilde{C}_{\mathbf{k}_m} = \sqrt{\frac{2\pi\hbar}{c|\mathbf{k}_m|}}\, \omega_{k_x} \mu_{cv} F_{\mathrm{ex}}(0) \times \int_{2D} d\boldsymbol{\rho}\, f_{\mathrm{ex}}(\boldsymbol{\rho}) e^{ik_y y + ik_{z,m} z}. \tag{41}$$

From this Hamiltonian we may obtain the radiative width of the excitons using the Fermi golden rule

$$\Gamma_{k_x,k_z} = \frac{\pi}{\hbar} \sum_{k_y,m} \frac{1}{DL_y} |\tilde{C}_{\mathbf{k}_m}|^2 \delta(\hbar c|\mathbf{k}_m| - \hbar\omega_{k_x}), \tag{42}$$

which after performing the summation on k_y as an integral becomes

$$\Gamma_{k_x,k_z} \simeq \sum_m \frac{2\pi\omega^2_{k_x}\mu^2_{cv}F^2_{\mathrm{ex}}(0)}{\hbar c^2 D\sqrt{\bar{k}^2 - k^2_{z,m}}}\, \theta(\bar{k}^2 - k^2_{z,m}). \tag{43}$$

where θ is the Heaviside function and $\bar{k}^2 = \omega^2_{k_x}/c^2 - k^2_x$.

The result of Eq. (43) is physically clear. Let us consider all the wire excitons in phase, i.e., $k_z = 0$. Then, if the grating is sufficiently closely packed, that is, when $D < 2\pi c/\omega$, the system behaves as if it were bidimensional and the exciton decays along two possible directions only, $k_y = \pm\bar{k}$, as in the QW case.[18–20] The radiative broadening also scales as $1/k_yD$, as previously found for the reflectivity.[21] This result is of course expected from elementary considerations on the scattering cross section of the wires, which is of the order of the wavelength of the light at the resonance, and on the density of the wires in the array configuration, which goes as $1/D$. The numerical value of the broadening also corresponds to the two-dimensional broadening of a QW having $|F_{\mathrm{ex,QW}}(0)|^2 = |F_{\mathrm{ex}}(0)|^2/D$. This also means that in the limit of close-packed wires the short lifetimes of two-dimensional excitons could be recovered.[22]

In the opposite case of loose-packed gratings, photon modes with $m \neq 0$ are also emitted in the decay of the exciton. We notice that even if more decay channels are present in this case, the lifetimes are longer than in the

previous close-packed case, because of the $1/D$ factor in Eq. (43). However, in this case an interesting resonant behavior is found in the radiative broadenings: divergences are found in Γ when the spacing of the wires corresponds to an integer number of wavelengths along z. These divergences correspond to those also found in the imaginary parts of the $\Sigma_i(k_x)$ as shown in Fig. 4.

Finally, we notice that a vanishing radiative broadening is obtained in the case of close-packed gratings when $k_z > \omega_0/c$; these modes are therefore similar to the QW surface polaritons already found.[18–20] However, they lack any center of mass dispersion along z, so that their dispersion is completely given by electromagnetic effects. Part of this dispersion is found from the real part of the grating-exciton self-energy. This is the most important contribution in the region of polariton dispersion that is close to the photon dispersion. Another part, as we have remarked before, originates from nonretarded interactions. The peculiar effect to notice about these surface modes is that they are guided modes with an efficient coupling of electromagnetic energy along a direction, without mobility of the electronic excitation along the same direction. This property may lead to interesting applications.

VI. CONCLUSIONS

We solve the problem of the scattering of an electromagnetic wave from a planar array of equispaced cylindrical scatterers with strong resonances and calculate the reflectivity of an array of quantum wires. We find that the effects of the electromagnetic interference between the wires generate additional shifts and broadenings of the isolated wire resonances. In order to quantitatively determine the magnitude of these effects, we analyze in detail some commonly used experimental configurations, when the incidence plane is parallel or perpedicular to the wire axis. Shifts in the meV range are expected in GaAs based structures, depending on the interwire distance. These shifts may be evidenced by changing the incidence angle in the case of a plane of incidence orthogonal to the wires or changing the polarization in the case of a plane of incidence perpendicular to the wires. Even at normal incidence, we argue that the shift for polarization along the wire may not be safely neglected in a closely packed grating, as the GaAs based gratings could be with an interwire separation of less than 200 nm. Resonance shifts and broadenings can also be qualitatively interpreted as properties of the mixed modes of the quantized electromagnetic fields and the full grating excitations, i.e., as grating polaritons. Surface modes typical of this array configuration could lead to interesting applications. These modes have confined electromagnetic energy in one direction, propagate in another, but are sustained by confined one-dimensional electronic excitations.

We hope to have given reasonable arguments to show that a mutual electromagnetic interference between the wires consitutes an interesting phenomenon that has to be taken into account in many real QG structures and could be also used to advantageously tune the electromagnetic properties (radiative lifetimes, exciton energy shifts, etc.) of nanostructures.

ACKNOWLEDGMENTS

The authors are indebted to R. Cingolani, A. D'Andrea, and R. Del Sole for useful discussions. They are also grateful to L. C. Andreani for valuable suggestions.

APPENDIX

We calculate the projection coefficients $\mathcal{S}$, the source coefficients $\epsilon_{\rm inc}^{\rm source}$, and the integrals of the Hankel functions over a line in the plane, all defined and used in the text. The key point is to observe that a solution of the scalar wave equation $(\nabla^2 + k^2)\psi = 0$ in a region R of the plane can be expressed as a superposition of solutions of different kind in the same region, for example, plane waves or cylindrical waves with different centers of the coordinate system. The same is also true for the *vector* equation in the plane. In order to calculate $\mathcal{S}$, we use this property to express an outgoing cylindrical wave from a center P' as a series of incoming and outgoing cylindrical waves centered in another point P,

$$H'_m(k\rho')e^{im'\phi'} = \sum_m c_{mm'} J_m(k\rho)e^{im\phi},$$

$$\rho < \text{distance between}(P \text{ and } P') = D. \quad \text{(A1)}$$

The coefficients $c_{mm'}$ may be calculated by a simple integration around any circumference of radius $R < D$,

$$c_{mm'} J_m(kR) = \frac{1}{2\pi}\int_0^{2\pi} d\phi e^{-im\phi} Z'_m[k\rho'(R,\phi)]e^{im'\phi'(R,\phi)}; \quad \text{(A2)}$$

this integration may be analytically carried out by using the limit of small R and the Taylor expansions for the Bessel functions. Carrying out the same calculation for a vector field, whose solutions were already given in Eq. (2), we find that the coefficients $c_{mm'}$ are connected $c_{mm'} = c_{|m-m'|}$ and finally

$$\mathcal{S}_{mim'i'} = \delta_{ii'} H_{|m-m'|}(kD). \quad \text{(A3)}$$

When we regard a *plane wave* as a superposition of cylindrical waves, starting from the well-known result for the scalar field[8]

$$e^{iky} = \sum_m J_m(k\rho)e^{im\phi}, \quad \text{(A4)}$$

where $y = \rho\sin\phi$, we obtain the projections coefficients for a generic plane wave reported in Eqs. (22) and (23). The integration formulas for the Hankel functions are instead obtained by regarding a *cylindrical wave* as a superpositon of plane waves (in a region R excluding the origin, e.g., a half plane)

$$H_m(k\rho)e^{im\phi} = \int_{-\infty}^{+\infty} dk_z \sum_i c_m(k_z) e^{ik_z z} e^{ik_y y_0} \qquad \text{(A5)}$$

and $\rho = \sqrt{y_0^2 + z^2}$, $e^{i\phi} = (z + iy_0)/\rho$, $k_y = \sqrt{k^2 - k_z^2}$, $y_0 > 0$, and $\mathrm{Im}(k_y) > 0$. The coefficients $c_0(k_z)$ may be calculated from an identity given in Ref. 8, taking the limit $y_0 \to 0$, and the other coefficients considering the vectorial expansion, so that one finally obtains

$$\int dz\, e^{-ik_z z} H_m(k\rho) e^{im\phi} = \frac{2e^{ik_y y_0}}{k_y} e^{-im\beta}, \qquad \text{(A6)}$$

with β already introduced before.

[1] A. Forchel, B. E. Maile, H. Leier, and R. Germann, in *Physics and Technology of Submicron Structures*, Proceedings of the V International Winter School, Mautendorf, Austria, edited by H. Heinrich, G. Bauer, and F. Kuchar (Springer, Berlin, 1988); S. Tsukamoto, Y. Nagama, M. Nishioka, and Y. Arakawa, J. Appl. Phys. **71**, 533 (1992); M. S. Miller, C. E. Pryor, H. Weman, L. A. Somoska, H. Kroemer, and P. M. Petroff, J. Cryst. Growth **111**, 323 (1991); D. Gershoni, J. S. Weiner, S. N. G. Chu, G. A. Baraff, J. M. Vandenberg, I. N. Pfeiffer, K. West, R. A. Logan, and T. Tanbun-Ek, Phys. Rev. Lett. **65**, 1631 (1990).

[2] R. Cingolani and R. Rinaldi, Riv. Nuovo Cimento **16**, (1993).

[3] A. D'Andrea and R. Del Sole, Phys. Rev. B **46**, 2363 (1992).

[4] R. Cingolani, K. Ploog, A. Cingolani, C. Moro, and M. Ferrara, Phys. Rev. B **42**, 2893 (1990); M. Kohl, D. Heitmann, P. Grambow, and K. Ploog, *ibid.* **42**, 2941 (1990).

[5] D. S. Citrin, Phys. Rev. B **50**, 5497 (1994).

[6] V. M. Agranovich, in *Surface Excitations*, edited by V. M. Agranovich and R. Loudon (North-Holland, Amsterdam, 1984), p. 557.

[7] E. Snitzer, J. Opt. Soc. Am. **51**, 491 (1961); see also F. E. Borgnis and C. H. Papas, in *Electromagnetic Waveguides and Resonators*, edited by S. Flügge, Encyclopaedia of Physics Vol. XVI (Springer-Verlag, Berlin, 1958).

[8] I. S. Gradshteyn and I. M. Ryzhik, *Tables of Integrals, Series and Products* (Academic, San Diego, 1980).

[9] F. Tassone and F. Bassani, Nuovo Cimento D **14**, 1241 (1992).

[10] P. Sercel and K. S. Vahala, Phys. Rev. B **42**, 3690 (1990); **44**, 5681 (1991).

[11] We notice that this equation has *homogeneous* solutions at eigenfrequencies $\omega(k_z)$, which correspond to modes confined in the grating, with $k_z > k_0$. These modes are also described in Sec. V; the reflectivity is not influenced by them because incoming and outgoing waves have $k_z < k_0$ and the modes cannot be coupled to them.

[12] F. Tassone, F. Bassani, and L. C. Andreani, Phys. Rev. B **45**, 6023 (1992).

[13] L.C. Andreani, Phys. Lett. A **192**, 99 (1994).

[14] D. Fröhlich, P. Köhler, E. Meneses-Pacheco, G. Khitrova, and G. Weimann, in *Proceedings of the International Meeting on the Optics of Excitons in Confined Systems*, edited by A. D'Andrea, R. Del Sole, R. Girlanda, and A. Quattropani (Institute of Physics, Bristol, 1992).

[15] B. S. Wang and J. L. Birman, Phys. Rev. B **43**, 12 458 (1991).

[16] D. S. Citrin, Phys. Rev. B **49**, 1943 (1994).

[17] D. S. Citrin, IEEE J. Quantum Electron. **29**, 2117 (1993).

[18] V. M. Agranovich and O. A. Dubovskii, Pis'ma Zh. Eksp. Teor. Fiz. **3**, 345 (1966) [JETP Lett. **3**, 223 (1966)].

[19] L. C. Andreani and F. Bassani, Phys. Rev. B **41**, 7536 (1990).

[20] F. Tassone, F. Bassani, and L. C. Andreani, Nuovo Cimento D **12**, 1673 (1990).

[21] It is to be noticed that this divergence for $k_y \to 0$, when the radiative broadening becomes larger than the resonant energies, is an artifact produced by the fixed pole approximation of the Fermi golden rule. However, it remains a fingerprint of a coupling of the excitations to a one-dimensional photon continuum, therefore of the recovery of a two-dimensional behavior of the excitations.

[22] D. S. Citrin, Phys. Rev. Lett. **69**, 3393 (1992).